Quarterly Technical Report

Selected Energy Epitaxial Deposition and Low Energy Electron Microscopy of AlN, GaN and SiC Thin Films

Supported under Grant #N00014-95-1-0122
Office of the Chief of Naval Research
Report for the period 1/1/96–3/31/96

R. F. Davis, H. H. Lamb† and I. S. T. Tsong*,
E. Chen†, R. Chilukuri†, R. B. Doak*, N. Freed*, J. Fritsch*,
C. Linsmeier*, M. Meloni*, V. Torres*, and S. Zhang
Materials Science and Engineering Department
†Chemical Engineering Department
North Carolina State University
Campus Box 7907
Raleigh, NC 27695-7907
and
*Department of Physics and Astronomy
Arizona State University
Tempe, AZ 85287-1504

March, 1996

REPORT DOCUMENTATION PAGE

Form Approved
OMB No. 0704-0188

1. AGENCY USE ONLY *(Leave blank)*	2. REPORT DATE	3. REPORT TYPE AND DATES COVERED
	March, 1996	Quarterly Technical 1/1/96–3/31/96

4. TITLE AND SUBTITLE

Selected Energy Epitaxial Deposition and Low Energy Electron Microscopy of AlN, GaN, and SiC Thin Films

5. FUNDING NUMBERS

1213801---01
312
N00179
N66020
4B855

6. AUTHOR(S)

R. F. Davis, H. H. Lamb and I. S. T. Tsong

7. PERFORMING ORGANIZATION NAME(S) AND ADDRESS(ES)

North Carolina State University
Hillsborough Street
Raleigh, NC 27695

8. PERFORMING ORGANIZATION REPORT NUMBER

N00014-95-1-0122

9. SPONSORING/MONITORING AGENCY NAMES(S) AND ADDRESS(ES)

Sponsoring: ONR, Code 312, 800 N. Quincy, Arlington, VA 22217-5660
Monitoring: Administrative Contracting Officer, Regional Office Atlanta
Regional Office Atlanta, 101 Marietta Tower, Suite 2805
101 Marietta Street
Atlanta, GA 30323-0008

10. SPONSORING/MONITORING AGENCY REPORT NUMBER

11. SUPPLEMENTARY NOTES

12a. DISTRIBUTION/AVAILABILITY STATEMENT

Approved for Public Release; Distribution Unlimited

12b. DISTRIBUTION CODE

13. ABSTRACT *(Maximum 200 words)*

Gallium nitride has been deposited using hyperthermal and thermal beams of NH_3 and triethylgallium seeded in He and Ar supersonic jets, respectively. The V/III ratio = 344. The growth rates were lower and the film character poor when Ar was used as the carrier. The films deposited using He were continuous and adherent and exhibited a characteristic wavy surface morphology. The major components of a new SEED facility have been received and verified. In research regarding direct ion beam deposition of GaN, it has been determined that ion current densities for N_2^+ at 10 and 20 eV using a Colutron ion beam unit are an order of magnitude higher at the latter energy; the peak current density at 20 eV is ~200 nA cm^{-2}, which corresponds to ~10^{-3} ML/sec deposition rate. The time of flight technique has been employed to characterize the intensity, energy, energy spread, and composition of a 10% NH_3 seeded He supersonic beam between 200 and 600°C and as a function of stagnation pressure and beam diameter. Clustering played a major role in determining the mean kinetic energy, as well as the energy spread. Initial density-functional calculations focused on the construction of various pseudopotentials for Ga involving the core states have been made to determine a proper treatment of the Ga d shell.

14. SUBJECT TERMS

selected energy deposition, SEED, supersonic jets, gallium nitride, Colutron, peak current density, time of flight, supersonic beams, stagnation pressure, beam diameter, clustering, kinetic energy, density functional calculations

15. NUMBER OF PAGES

21

16. PRICE CODE

17. SECURITY CLASSIFICATION OF REPORT	18. SECURITY CLASSIFICATION OF THIS PAGE	19. SECURITY CLASSIFICATION OF ABSTRACT	20. LIMITATION OF ABSTRACT
UNCLAS	UNCLAS	UNCLAS	SAR

Table of Contents

I. Introduction

The realized and potential electronic applications of AlN, GaN and SiC are well known. Moreover, a continuous range of solid solutions and pseudomorphic heterostructures of controlled periodicities and tunable bandgaps from 2.3 eV (3C-SiC) to 6.3 eV (AlN) have been produced at North Carolina State University (NCSU) and elsewhere in the GaN-AlN and AlN-SiC systems. The wide bandgaps of these materials and their strong atomic bonding have allowed the fabrication of high-power, high-frequency and high-temperature devices. However, the high vapor pressures of N and Si in the nitrides and SiC, respectively, force the use of low deposition temperatures with resultant inefficient chemisorption and reduced surface diffusion rates. The use of these low temperatures also increases the probability of the uncontrolled introduction of impurities as well as point, line and planar defects which are likely to be electrically active. An effective method must be found to routinely produce intrinsic epitaxial films of AlN, GaN and SiC having low defect densities.

Recently, Ceyer [1, 2] has demonstrated that the barrier to dissociative chemisorption of a reactant upon collision with a surface can be overcome by the translational energy of the incident molecule. Ceyer's explanation for this process is based upon a potential energy diagram (Fig. 1) similar to that given by classical transition-state theory (or activated-complex theory) in chemical kinetics. The dotted and dashed lines in Fig. 1 show, respectively, the potential wells for molecular physisorption and dissociative chemisorption onto the surface. In general, there will be an energy barrier to overcome for the atoms of the physisorbed molecule to dissociate and chemically bond to the surface. Depending upon the equilibrium positions and well depths of the physisorbed and chemisorbed states, the energy of the transition state E^* can be less than zero or greater than zero. In the former case, the reaction proceeds spontaneously. In the latter case, the molecule will never proceed from the physisorbed state (the precursor state) to the chemisorbed state unless an additional source of energy can be drawn upon to surmount the barrier. This energy can only come from either (1) the thermal energy of the surface, (2) stored internal energy (rotational and vibrational) of the molecule, or (3) the incident translational kinetic energy of the molecule. Conversion of translational kinetic energy into the required potential energy is the most efficient of these processes. Moreover, by adjusting the kinetic energy, E_i, of the incoming molecule, it is possible to turn off the reaction ($E_i < E^*$), to tailor the reaction to just proceed ($E_i = E^*$), or to set the amount of excess energy to be released ($E_i > E^*$). The thrust of the present research is to employ these attributes of the beam translational energy to tune the reaction chemistry for wide bandgap semiconductor epitaxial growth.

The transition state, E^*, is essentially the activation energy for dissociation and chemisorption of the incident molecules. Its exact magnitude is unknown, but is most certainly

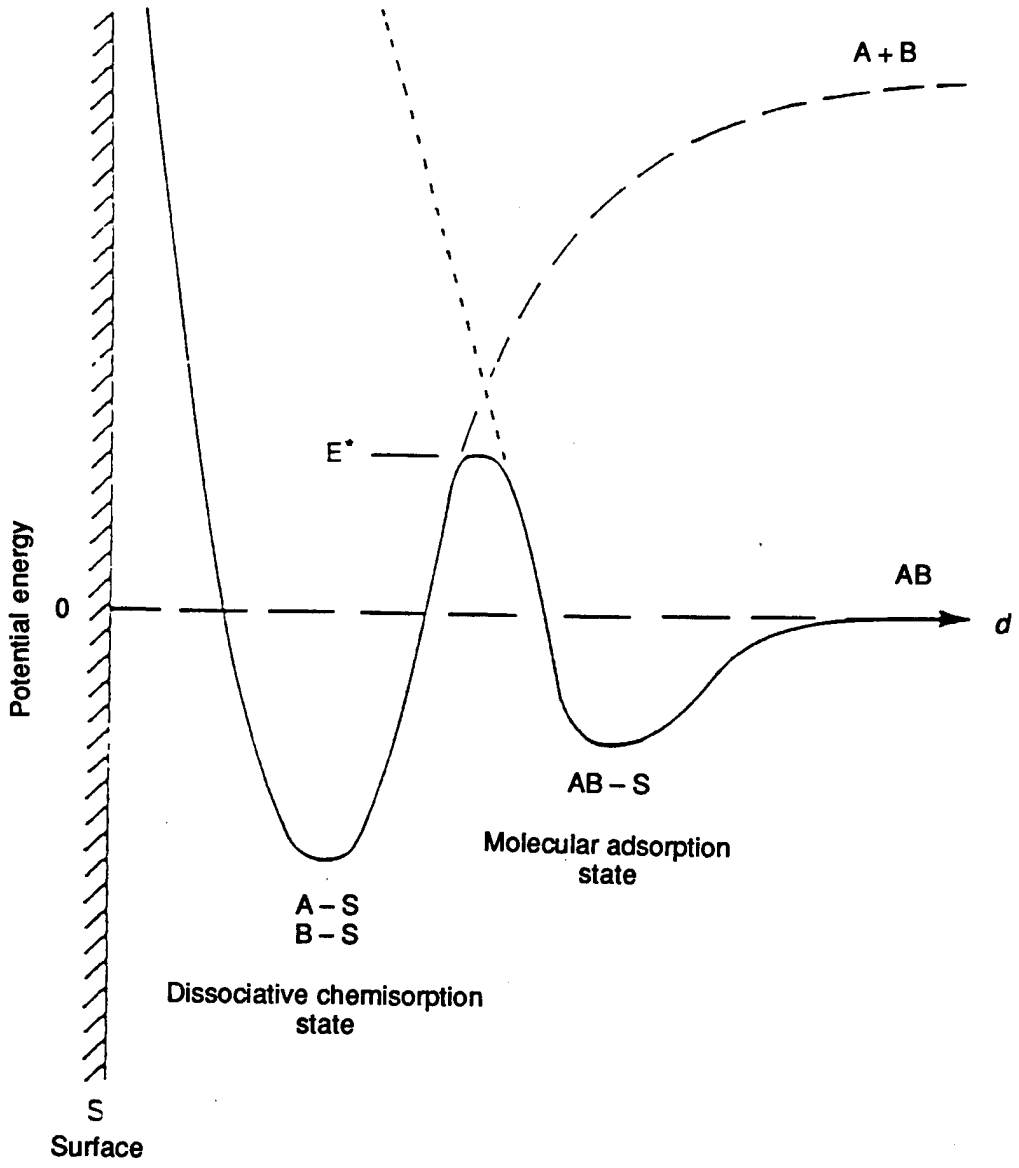

Figure 1. Schematic potential energy diagram of an activated surface reaction involving a molecularly physisorbed precursor state [from Ref. 1].

lower than the dissociation energy of the free molecule. It does not necessarily follow, however, that any kinetic energy above E^* will promote high-quality epitaxial growth of GaN. One must take into consideration another energy threshold, E_d, beyond which the kinetic energy of the incident flux will cause damage to the epitaxial film being synthesized. A typical E_d threshold value is approximately five times the bandgap of the crystal and in the case of GaN, $E_d \approx 18$ eV.

From the above consideration, it is clear that the key to high quality epitaxial growth is to be able to tune the energy of the incoming flux species over a range of energies defined by the window between E^* and E_d. Since the window is quite restrictive, i.e. 1-20 eV, it is essential

that the energy spread of the flux species must be small, i.e. the flux species should ideally be monoenergetic. To this end, we employ Selected Energy Epitaxial Deposition (SEED) systems for the growth of AlN, GaN and SiC wide bandgap semiconductors. The SEED systems are of two types: (1) a seeded-beam supersonic free-jet (SSJ) and (2) a dual ion-beam Colutron. Both these SEED systems have the desirable property of a narrow energy spread of ≤ 1 eV.

Epitaxial growth using the seeded-beam SSJ involves a close collaboration between investigators at NCSU and Arizona State University (ASU). At ASU, the SSJ is interfaced directly into a low-energy electron microscope (LEEM) for the conduct of *in situ* studies of the nucleation and growth of epitaxial layers; while at NCSU, the SSJ systems are used to grow device-quality AlN, GaN and SiC for real applications. Exchanges in personnel (students) and information between the two groups ensures the achievement of desired results. The additional thin film growth experiments using dual-beam Colutrons and the theoretical studies referred to in this report are primarily conducted at ASU.

The research conducted in this reporting period and described in the following sections has been concerned with (1) deposition of GaN using hyperthermal and thermal beams of NH_3 and triethylgallium seeded in He and Ar supersonic jets, respectively, (2) determination of N_2^+ ion current densities using a Colutron ion beam unit, and (3) the use of the time of flight technique to characterize the intensity, energy, energy spread, and composition of a 10% NH_3 seeded He supersonic beam between 200 and 600°C and as a function of stagnation pressure and beam diameter, and (4) density-functional calculations which were focused on the construction of various pseudopotentials for Ga involving the core states to determine a proper treatment of the Ga d shell. The following individual sections detail the procedures, results, discussions of these results, conclusions and plans for future research. Each subsection is self-contained with its own figures, tables and references.

1. S. T. Ceyer, Langmuir 6, 82 (1990).
2. S. T. Ceyer, Science 249, 133 (1990).

II. Selected Energy Epitaxial Deposition of Gallium Nitride

A. Introduction

The III-V nitrides and SiC are promising optoelectronic materials with direct band gaps in the 2.3 to 6.3 eV range. Gallium nitride, which has a band gap of 3.4 eV, is currently employed in the commercial fabrication of light emitting diodes (LEDs) and laser diodes (LDs) operating in the blue and ultraviolet regions.

Epitaxial growth of high-quality monocrystalline GaN thin films has been problematic due to the lack of a suitable lattice-matched substrate and the thermodynamic instability of the material under high-temperature chemical vapor deposition (CVD) conditions. For sapphire, the most common substrate, there is a 16% lattice mismatch at the α-GaN (0001)/sapphire (0001) interface; however, by employing a low-temperature AlN or GaN buffer layer one can obtain defect densities in the 10^8–10^9 cm^{-2} range. In conventional CVD using $GaCl_3$ and NH_3 or metal-organic CVD (MOCVD) using $Ga(CH_3)_3$ and NH_3, substrate temperatures of 1000-1100°C are required to overcome the activation energy barrier for dissociative chemisorption of NH_3 and provide thermal energy for adatom surface diffusion [1]. Such high growth temperatures are undesirable since GaN is thermally unstable above 620°C *in vacuo* [2]. Consequently, the as-deposited films typically have high conductivities owing to n-type doping via oxygen impurities or N vacancies.

Plasma-assisted processes have been utilized to lower the GaN growth temperature to 600-700°C, but ion-induced damage and oxygen contamination are often observed. The use of energetic neutral beams of precursor molecules is an alternative approach to the epitaxial growth of GaN films at lower substrate temperatures. In selected energy epitaxial deposition (SEED), heavy reactant molecules are seeded in a supersonic expansion of light molecules and thereby accelerated to hyperthermal energies. The precursor molecules attain kinetic energies on the order of several eV which can provide the necessary energy for activated surface processes, such as dissociative chemisorption and adatom migration. Hence, in prospect, monocrystalline GaN films may be grown at much lower substrate temperatures by SEED than by conventional thermal techniques [4]. Moreover, energetic neutral beams with narrow energy distributions will be useful in fundamental studies of wide bandgap semiconductor growth using *in situ* low-energy electron microscopy (LEEM) and other techniques.

As discussed in previous reports (Sept. 1995, Dec. 1995), GaN thin films have been deposited on sapphire(0001) via SEED at 600°C using V/III ratios ≥200 [5]. This report documents further progress in our efforts to elucidate the effects of precursor incident translational energy on growth kinetics and film morphology. A status report on the new seeded molecular beam deposition facility is included.

B. Experimental Procedure

Films were grown using dual supersonic free jets of NH_3 and TEGa seeded in He or Ar using the reactor system described in the previous report (Dec., 1995). Research grade He or Ar was used as the carrier (or bath) gas for the precursor molecules. The NH_3 nozzle was heated to 550°C and the TEGa nozzle was unheated. Typical operating conditions are given in Table I.

Table I. Comparison of SEED Conditions using He and Ar

Parameter	He Carrier	Ar Carrier
NH_3 jet stagnation pressure	800 Torr	≥2160 Torr*
NH_3 flow rate	12 sccm	12 sccm
NH_3 carrier flow rate	240 sccm	240 sccm
Vol% NH_3 in carrier	5%	5%
TEGa bubbler pressure	860 Torr	1020 Torr
TEGa bubbler temperature	-10°C	3°C
TEGa carrier flow rate	40 sccm	20 sccm
TEGa flow rate	0.034 sccm	0.035 sccm
Vol% TEGa in carrier	0.085 %	0.176 %
NH_3 : TEGa ratio	354	344

* estimated value

The samples were transferred to a UHV chamber equipped for Auger electron spectroscopy (AES), and Ar^+ milled prior to surface analysis. The AES was performed with a primary electron energy of 3 keV and data was collected for 10 ms at each 1 eV scanning step for 10 iterations. SEM images were obtained using a JEOL 6400 field emission scanning electron microscope operated with a 5 keV primary beam.

C. Results and Discussion

Seeding in He and Ar. In an ideal supersonic expansion (e.g. perfect gas behavior, zero velocity slip, infinite Mach number), the average kinetic energy of an individual molecular species in a mixture of average molecular weight, W_{ave}, is given by:

$$\langle E_i \rangle = \frac{W_i}{W_{ave}} \frac{\gamma R T_0}{(\gamma-1)}$$

where, γ, R, T_0 and W_i are the molar heat capacity ratio C_p/C_v, the gas constant, the gas stagnation temperature and the molecular weight of the individual species, respectively. Heavy molecules seeded in a lighter gas achieve higher translational energies than in a pure heavy gas expansion. Conversely, light molecules seeded in a heavier bath gas are slowed down. For example, NH_3 seeded at 5 vol% in He and expanded from a 550°C nozzle will attain an average kinetic energy of 0.64 eV. In contrast, 5% NH_3 seeded in Ar and expanded under similar conditions will result in an average NH_3 kinetic energy of only 0.08 eV. In comparison, the average kinetic energy of an 550°C effusive NH_3 beam is 0.07 eV. Thus, by substituting Ar for He as the bath gas, the NH_3 translational energy can be switched from the hyperthermal to the thermal regime. Similarly, the average kinetic energy of TEGa molecules seeded at 0.1 vol% in He and expanded from a 25°C nozzle is 2.44 eV. By substitution of Ar for He, the average TEGa translational energy is reduced to 0.25 eV.

One experimental consideration when switching from He to Ar as the carrier gas is the reduction of the nozzle throughput due to the lower sonic velocity, $V_s = (\gamma RT/W_{ave})^{1/2}$. For equivalent stagnation conditions and nozzle diameters, the molar flow rate ratio for monoatomic gases is given by, $[m_A/m_B] = [W_B/W_A]^{1/2}$. Consequently, to obtain equivalent reactant fluxes without increasing the nozzle diameter, the stagnation pressure must be increased.

Comparison of Films Deposited Using Hyperthermal and Thermal Beams. In the previous experiments (Dec., 1995), conditions were identified for deposition of highly oriented polycrystalline GaN films on sapphire(0001) at 600°C using hyperthermal beams of NH_3 and TEGa which were generated by seeding in He. In the present report, a comparison is made to a GaN film grown on sapphire(0001) at 600°C using NH_3 and TEGa seeded in Ar supersonic jets. The reactant fluxes were approximately equivalent to those used previously (Table I) giving a V/III ratio = 344. The film was deposited using the two-step nucleation/growth method described in the previous report. Qualitatively, the resultant film was distinctly different from the continuous, nearly transparent films deposited using hyperthermal beams; it was discontinuous with a yellow, powdery appearance.

Figure 1 compares the Auger electron spectra of films grown using He and Ar as the carrier gases illustrating that stoichiometric GaN is deposited on sapphire under these conditions, irrespective of incident kinetic energy of the precursors. Although both films show comparable N:Ga ratios, the SEM pictures reveal that the growth rates are lower and the film characteristics are poor when Ar is used as the carrier.

Figure 2 shows a top-view SEM of a GaN film grown at 600°C using NH_3 and TEGa seeded in He at V/III ratio of 354. The film is continuous and adherent and exhibits a characteristic wavy surface morphology. As reported previously, the cross-sectional image of this film and others deposited under similar conditions exhibit faceting and a columnar morphology. The growth rate is estimated at 0.75 μm/hr. RHEED patterns are consistent with

a polycrystalline film exhibiting a large degree of preferred crystallographic orientation. These results strongly support the feasibility of growing monocrystalline GaN films using hyperthermal molecular beams.

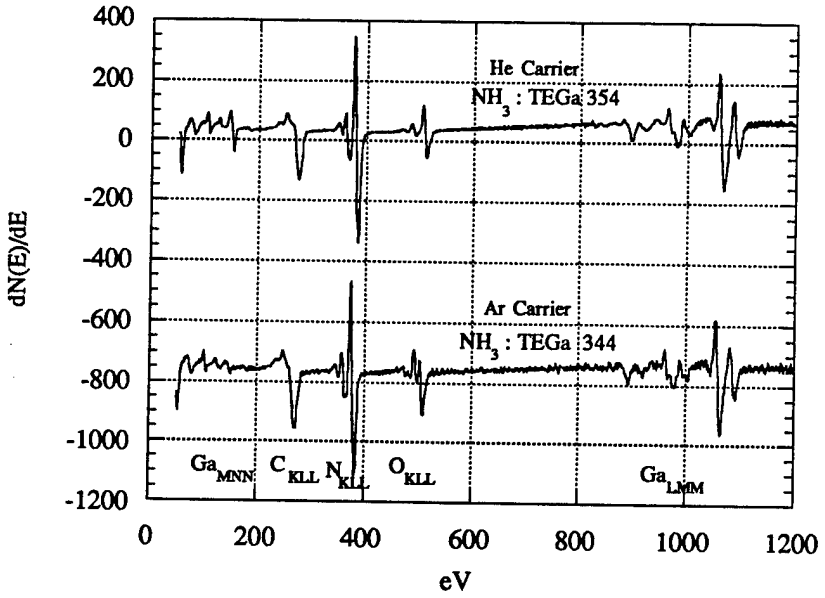

Figure 1. Auger electron spectra of GaN films grown using He and Ar as the seeding gases.

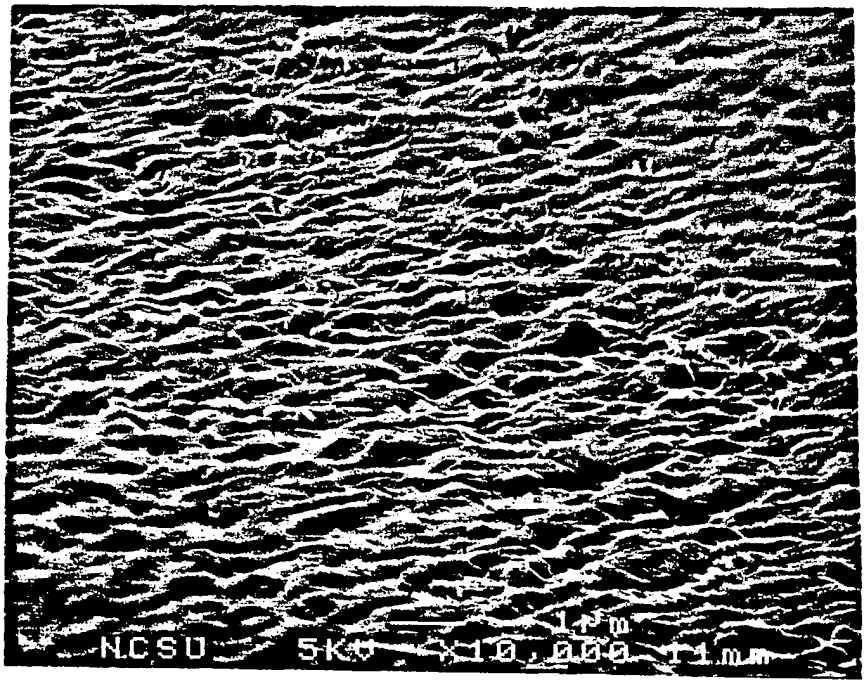

Figure 2. GaN film grown using He as the carrier gas.

In contrast, the film grown using Ar as the carrier gas exhibits a very different morphology, as illustrated in the SEM image of Fig. 3. The film is non-uniform and exhibits globules and helical whiskers that are indicative of excess Ga. Similar features are also observed on films grown under Ga-rich conditions (V/III ratios <200) using hyperthermal beams. They appear to form primarily due to insufficient nitridation of the nucleated Ga, which is consistent with a lower NH_3 sticking coefficient. The estimated growth rate of GaN with Ar as the carrier gas is 0.25 μm/hr, consistent with lower NH_3 reactivity.

The lower growth rate and poor quality of films grown with low-kinetic-energy beams (as reported here and in separate experiments reported in Dec., 1995) strongly support the working hypothesis that precursor incident kinetic energies in the hyperthermal regime can be used to optimize low-temperature epitaxial growth of GaN and other III-V nitrides.

Status of New SEED Facility. The major components for the new apparatus have arrived and have been verified. The status of each individual chamber is detailed below:

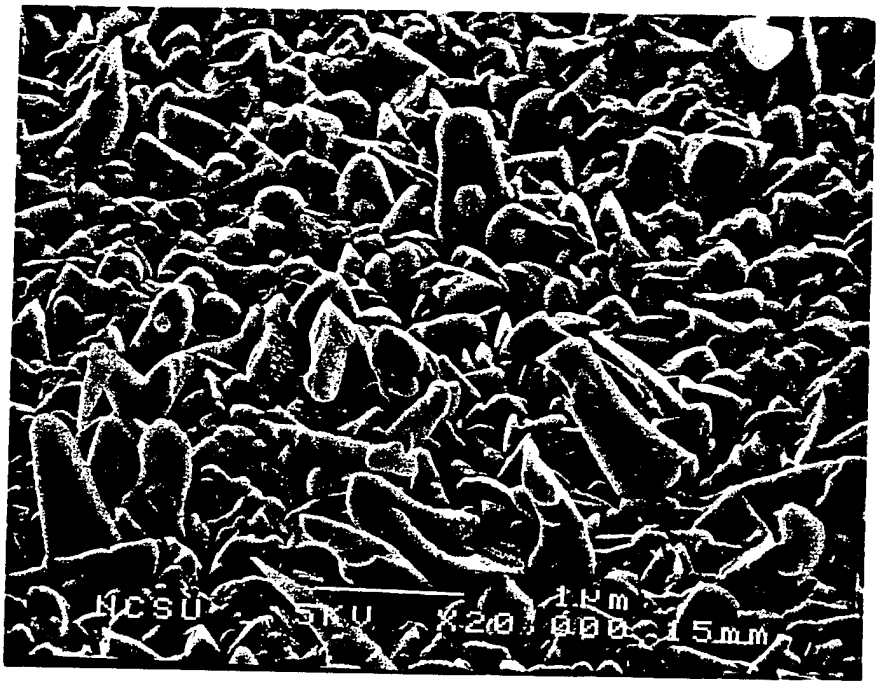

Figure 3. GaN film grown using Ar as the carrier gas.

Source Chamber:

1) A VHS-6 diffusion pump with a water-cooled baffle and a VHS-400 diffusion pump, both backed by mechanical pumps have been installed on the source chamber.
2) The chopper assembly design for TOF analysis has been finalized. High speed motors for beam choppers have arrived.
3) Nozzle assemblies that are heatable to 800°C and permit precise xyz positioning have been designed and are under construction.

Deposition Chamber:

1) RHEED gun and its accessories, a rotatable turntable with an elevator for the mass spectrometer, a titanium sublimation pump, and viewports have been installed on the deposition chamber, and the chamber has been tested to 1×10^{-9} Torr using a turbomolecular pump.
2) A sample heater assembly, designed for heating to 1000°C by using a boron nitride coated graphite heating element, is under construction.

Analysis Chamber:

1) Analysis chamber has been tested to 1×10^{-10} Torr using an ion pump and a TSP, and a sample manipulator has been installed.
2) XPS with 16-element multichannel detector and dual Al/Mg anode x-ray source is operational. Figures 4 and 5 are XP spectra of GaN films grown on sapphire substrates. The spectra were measured using the Al anode with the samples supported on Si wafers.

Miscellaneous:

1) The cryopump, gate valves, transfer rods and other components for the loadlock have arrived, and the loadlock is under construction.
2) The mass flow controllers, valves, fittings and other components for the gas flow system have arrived. The layout for the same has been finalized and the system is under construction.

D. Future Plans

1) Complete the construction of the gas flow system, the sample heater assembly, the nozzle assembly, the loadlock and the TOF system. (March - April, 1996)
2) Perform TOF analysis on TEGa and TMGa seeded in He supersonic expansions. (May, 1996)
3) Study the growth of AlN buffer layers using $Al(CH_3)_3$ and NH_3. (May-June, 1996)
4) Initial studies of GaN growth on sapphire using dual seeded supersonic molecular beams. (July-August, 1996)
5) Study the effect of seeding the precursor molecules in hydrogen. (August, 1996)

E. References

1. S. Nakamura, Japan J. Appl. Phys. **30**, L1705 (1991).
2. M. R. Lorenz and B. B. Binkowski, J. Electrochem Soc. **109**, 24 (1962).
3. H. P. Maruska and J. J. Tietjen, Appl. Phys. Lett. **15**, 327 (1969).
4. H. H. Lamb, K. K. Lai, V. Torres and R. F. Davis, in "Film Synthesis and Growth Using Energetic Beams," MRS Symp. Proc. **388** (1995).
5. J. J. Sumakeris, R. K. Chilukuri, R. F. Davis and H. H. Lamb, in "Gallium Nitride and Related Materials," MRS Symp. Proc. **395** (1996).

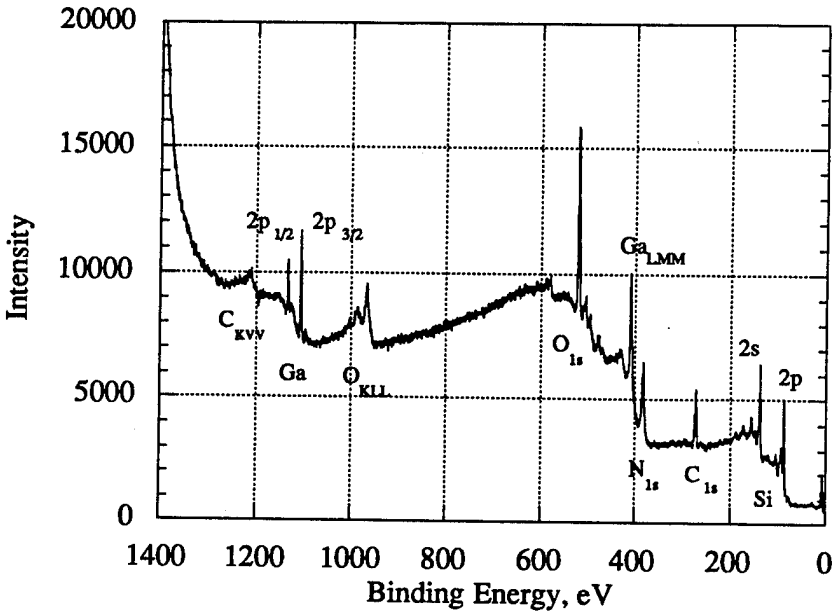

Figure 4. XPS spectrum of GaN film grown using He as the carrier gas.

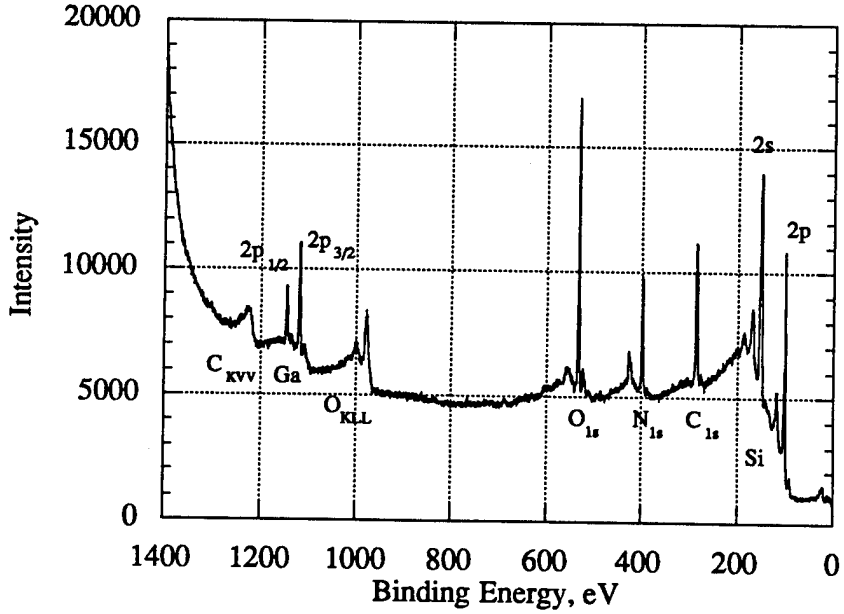

Figure 5. XPS spectrum of GaN film grown using Ar as the carrier gas.

III. Deposition by Dual Colutron Ion Beams

A. Introduction

The objective of this work is to produce epitaxial SiC and GaN films by direct ion-beam deposition of the two reacting chemical species. The deposition system consists of two Colutron ion beam units each equipped with a Wien Filter to select the mass of the desired ion, and an electrostatic deceleration lens to produce low-energy ions in the 10 eV range. The ion beams from the Colutron ion sources are near-monoenergetic, with an energy spread as low as 0.1 eV. The deposition system is further equipped with RHEED to monitor *in situ* film growth, a 4-grid retarding field analyzer to conduct LEED and AES to determine the surface structure and chemical composition of the films respectively, and an electrostatic energy analyzer to determine the energy distribution of the ions and also to characterize the composition of the top surface layer by ion-scattering spectrometry (ISS).

B. Experimental Procedure

We have used a Faraday cup with an 0.5 mm diameter opening to map out the spatial distribution of the ion current. The Faraday cup was mounted on a x-y-z manipulator directly in the path of the beam. The cup was moved in the z-x plane and the ion currents at specific energies were measured.

C. Results and Discussion

In Fig. 1, the current density of N_2^+ ions at 20 eV is an order of magnitude higher than that at 10 eV. The peak current density at 20 eV is ~200 nA cm^{-2}, which corresponds to ~10^{-3} ML/sec deposition rate. The current densities at 10 eV for N_2^+ (Fig. 1), N^+ and C^+ (Fig. 2) give deposition rates <10^{-4} ML/sec which are obviously too low. However, these current densities were obtained without any particular careful alignment of the Colutron ion beam system. The lack of alignment is obvious from the non-uniform beam profiles in Figs. 1 and 2. With proper alignment, we expect to achieve a Gaussian shape beam profile and a considerable enhancement in beam current.

E. Future Research and Goals

Both Colutron ion beam units will be aligned mechanically and electrostatically. The ion current distribution will be measured after the alignment procedure. Both solid ions such as Ga^+ and Si^+, and gaseous ions such as N_2^+, N^+ and C^+ (from CO), will be tested on the ion sources. It is hoped to achieve a deposition rate of at least 10^{-3} ML/sec for 10 eV ions, and 10^{-2} ML/sec for 20 eV ions. The energy distribution, i.e. spread, of each ion species will also be measured.

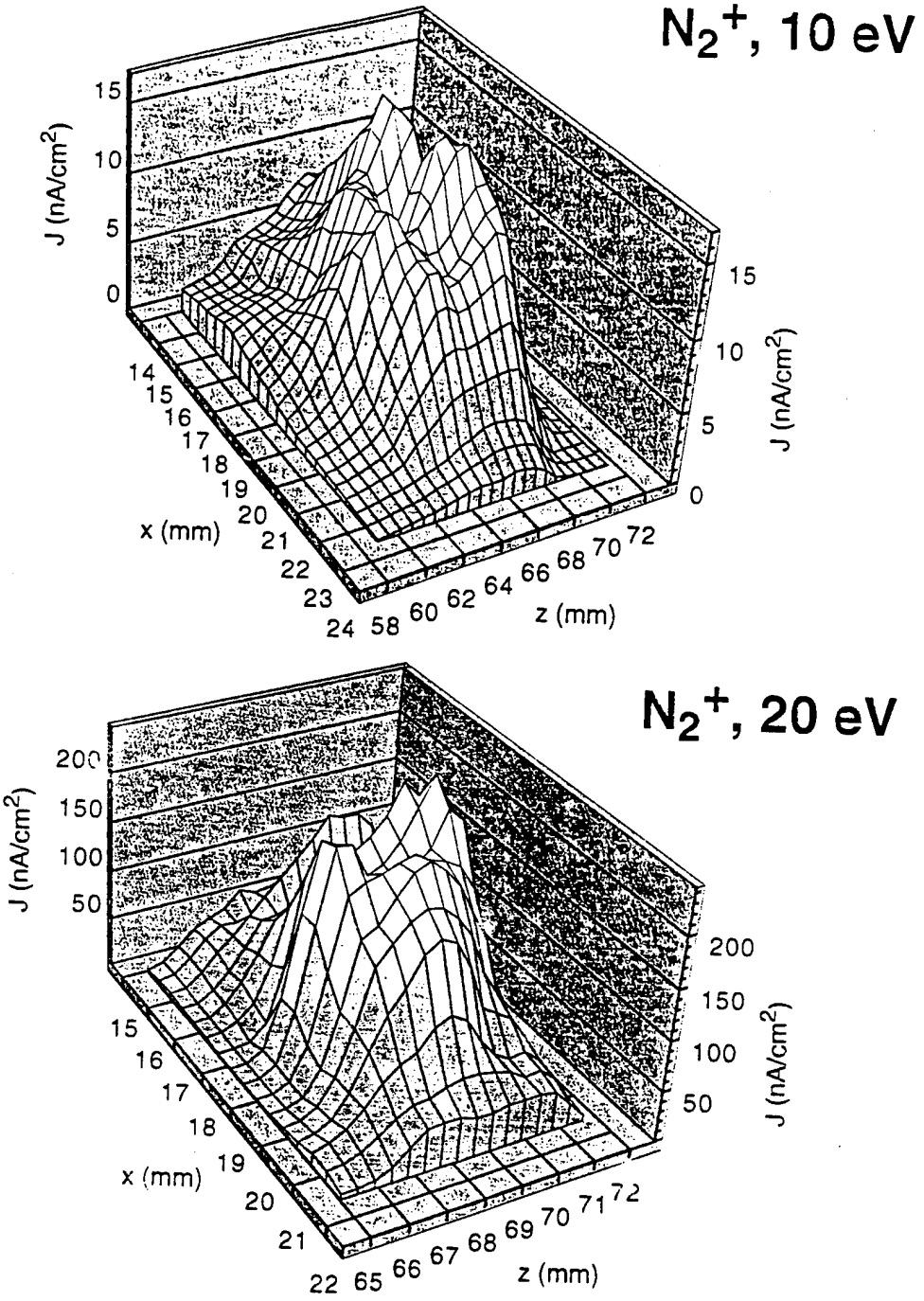

Figure 1. The ion current distributions for N_2^+ molecular ions at 10 eV and 20 eV.

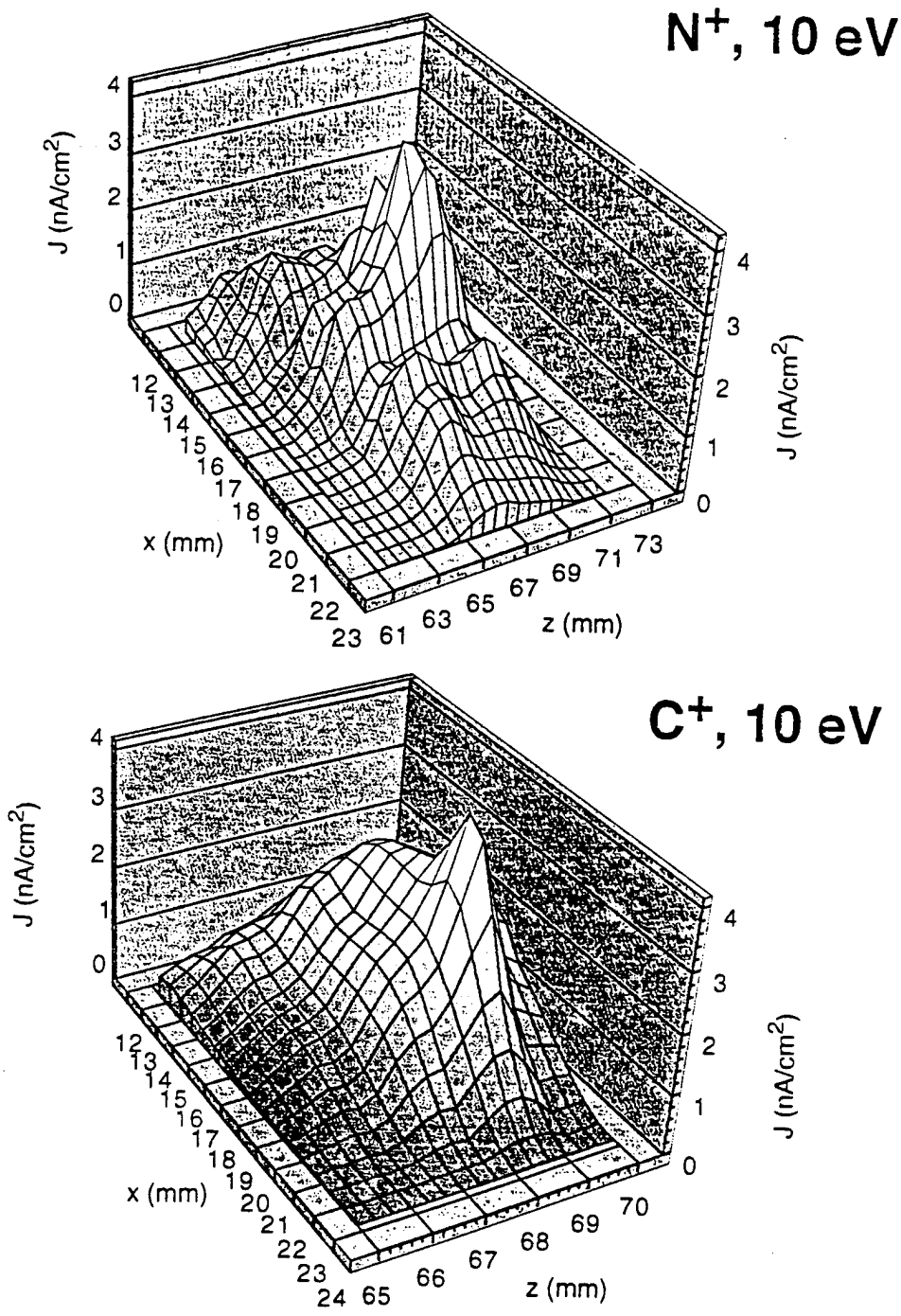

Figure 2. The current distributions for 10 eV N^+ and C^+ atomic ions.

IV. Testing of a NH_3 Seeded He Supersonic Molecular Beam Source for Growth of AlN and GaN Layers

A. Introduction

The nitride family of AlN, GaN and InN thin films have shown to be strong candidates for electronic and optoelectronic applications. With direct band gaps of 6.2 eV, 3.4 eV and 1.9 eV for AlN, GaN and InN, respectively, solid solutions based on these materials provide for band gap modifications suitable for applications ranging from the red to the deep UV region of the spectrum [1]. Due to the high bond strength between N and H in NH_3, the growth of III-V nitrides requires high substrate temperatures unless some other form of activation is present. Supersonic Molecular Beam Epitaxy (SMBE) has been shown to enhance the surface decomposition of silane and methane [2,3] because of the possibility of tuning the kinetic energy of these species to deform and cleave the bonds upon impact with the substrate. In addition, the tuning of the energy spread is possible with SMBE. This is important in order to experimentally determine the chemisorption barriers for the systems being studied, as well as to provide species with high sticking coefficients at high enough intensities. SMBE is, therefore, a useful technique for the low-temperature growth of single-crystalline GaN films at suitable growth rates using NH_3. A review of supersonic molecular beams can be found in Scoles [4].

The characterization of the mean kinetic energy, energy spread and composition as a function of stagnation pressure (P_o), stagnation temperature (T_o), and nozzle diameter (d) for NH_3 seeded He supersonic molecular beams has been performed.

B. Experimental Procedure

The Time of Flight (TOF) technique was used to characterize the beam intensity, energy, energy spread and composition as a function of P_o, d and T_o. Pt electron microscope apertures were used as orifices and they were calibrated by measuring the flux through the orifice as a function of pressure using a He calibrated Matheson flow meter. T_o was varied from 300K to 900K using an inconel coiled band heater. High pressure (HP) data were acquired with a nozzle diameter of 20 μm and a low pressures (LP) data with a nozzle diameter of 103 μm. This allowed us to determine the net effect of pressure and diameter independently. The HP series were performed using a tank pressurized at 1050 PSI of 10% NH_3 in He and a regulator to control the pressure. The pressure was read with a sensotec gauge transducer. The LP gas manifold has been described in previous reports. The TOF apparatus, as well as the calibration procedure, is described elsewhere [5].

To estimate the mean velocity (u) and velocity spread (Δu), a Gaussian fit of the following form was used:

$$F(v) = Av^2 \exp(-(\frac{v-u}{\Delta u})^2).$$

The background was subtracted from the data prior to the before fitting. The function parameters were modified until a residual greater than 0.99 was obtained. The integrated intensities of the beams were then calculated by integrating the Gaussian fit as follows:

$$I = \int_{400}^{4000} F(v)dv$$

where the limits of integration covered beyond the velocities of interest.

C. Results and Discussion

Figure 1 shows the HP mean kinetic energy as a function of P_od for values of T_o of 200°C, 400°C and 600°C. The scaling of mean kinetic energy with temperature is clearly shown. At 200°C, then mean kinetic energy seems to increase monotonically with P_od. At 400°C and 600°C the mean kinetic energies increase initially with P_od but seem to level off at 0.48 eV and 0.65 eV. Figure 1 also shows the LP mean kinetic energy and the HP mean kinetic energy as a function of P_od. At 200°C the LP data seems to be lower than the HP data for P_od greater than 25 Torr-cm while the opposite occurs for the 400°C data. The presence of clusters in these beams is thought to be the reason for this behavior. Fig. 2 shows the integrated intensity of the HP TOF spectra for T_O = 200, 400 and 600°C. There were no clusters detected at 600°C. Therefore, the integrated intensity should increase as a function of P_od in a linear fashion which is the case (see Fig. 2). At 400°C the integrated intensity is found to increase initially and then plateau and increase again. A similar behavior is found at 200°C. Clustering was detected with the mass spectrometer for 200°C and 400°C. Therefore, the loss in intensity for the monomer is due to clustering. As the temperature decreases during the expansion there must exist a minimum collision frequency for clustering which should also decrease. This minimum collision frequency will correspond to a higher temperature for the 400°C HP series relative to the 200°C LP series. Upon clustering the system gains energy from the release of the enthalpy of condensation and at the same time the average mass of the mixture increases. The amount of enthalpy gained is a function of the local beam temperature (T) where clustering occurs. Therefore, the final velocity of the beam can be rewritten in the following form to include dimers and real gas effects :

$$V_\infty = \sqrt{\frac{2\left(\frac{\gamma R(T_o - T)}{\gamma - 1} + \Delta H_{real} + x_d \Delta H_{cond.}\right)}{W}}$$

where ΔH_{real} is the real gas enthalpy, $\Delta H_{cond.}$ is the enthalpy of condensation and x_d is the mole fraction of dimmers. For the sake of modeling the differences in u for the HP and the LP data series, the temperature dependence of $\Delta H_{cond.}$ has to be considered. $\Delta H_{real.}$ is assumed to

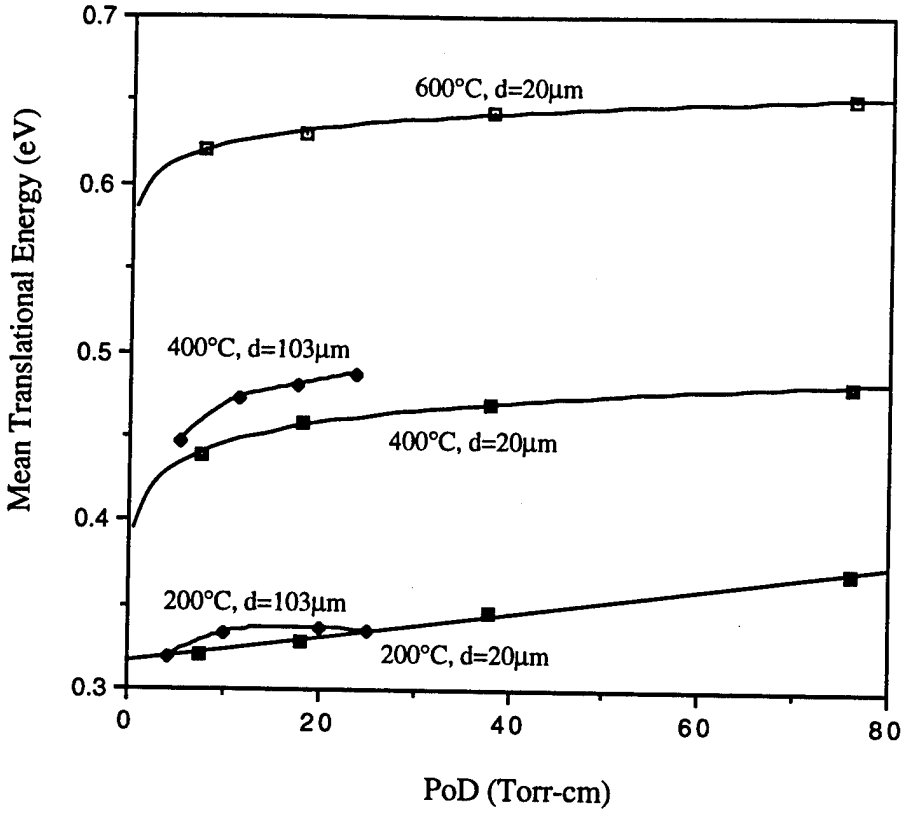

Figure 1. Mean kinetic energy as a function of the stagnation pressure-diameter product.

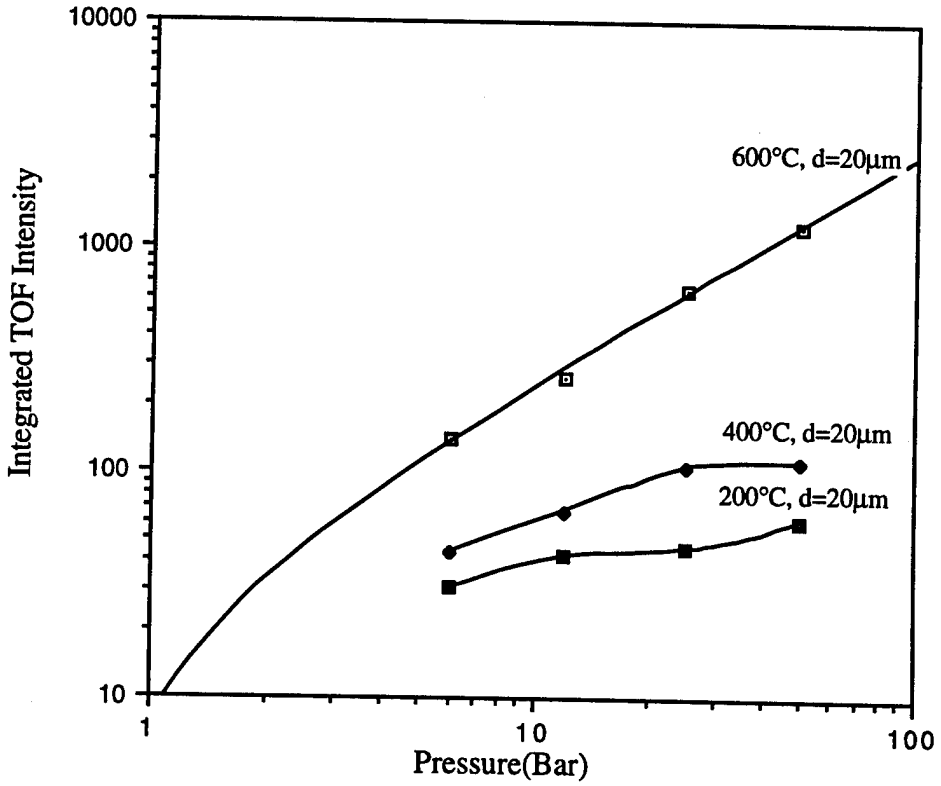

Figure 2. Integrated TOF intensity as a function of stagnation pressure.

be negligible in the following analysis although it explains the slow but continuous rise in energy as a function of P_od for the 600°C HP series. The ideal gas enthalpy decreases with decreasing temperature where as $\Delta H_{cond.}$ increases with decreasing temperature. We can rewrite V_∞ as :

$$V_\infty = A\sqrt{\frac{1+\alpha x_d}{W}}$$

where α is the ratio of the enthalpy of condensation and the ideal gas enthalpy and A is a constant. Figure 3 shows the temperature dependence of α which is linear and decreases with increasing temperature. The average molecular weight, W, can be rewritten to include dimers as:

$$W = \frac{0.9m_{He} + m_{NH_3}(0.1-2x_d) + m_{(NH_3)_2}x_d}{1-x_d}$$

where x_d is the mole fraction of dimers. In order to determine the effect of clustering on the beam energy as a function of local beam temperature T, we need to consider the sign of the derivative of V_∞ with respect to x_d at $x_d = 0$ as a function of T. Figure 4 shows a plot of this derivative with respect to T and it is clear that the temperature at which clustering occurs determines if V_∞ increases or decreases. This analysis is in perfect agreement with the dependence of clustering on P_o for the different temperatures. That is, that at 400°C the local beam temperature where clustering occurs is higher than at 200°C. Therefore, the HP series at 400°C is lower in energy than the LP series and the opposite occurs at 200°C.

As mentioned previously, the energy spread of the beam is related to the local beam temperature T. Figure 5 shows the energy spread (ΔE) as a function of P_od at various T_o. ΔE decreases as T_o decreases and P_od increases. The HP series shows a slower decrease in ΔE as P_od increases relative to the LP series. Beyond a given value of P_od, ΔE for the LP data is lower than that of the HP data. This trend can be explained by considering the interplay between clustering and cooling efficiency of the beam. The amount of clusters scales with P_o^2d [4]. This implies that more clusters are formed in the HP data. Clustering occurs much earlier in the expansion for the HP data and the enthalpy released is converted into kinetic energy more efficiently. As the pressure for the LP series is raised the onset of clustering moves closer to the nozzle and the extent of clustering increases. However, the beam is cooled more efficiently with increasing P_o resulting in a lower ΔE for the LP series relative to that of the HP data beyond a given value of P_od.

D. Conclusion

10% NH_3 seeded He supersonic molecular beams have been characterized for stagnation temperatures ranging from 200°C to 600°C and stagnation pressures and diameters. The mean

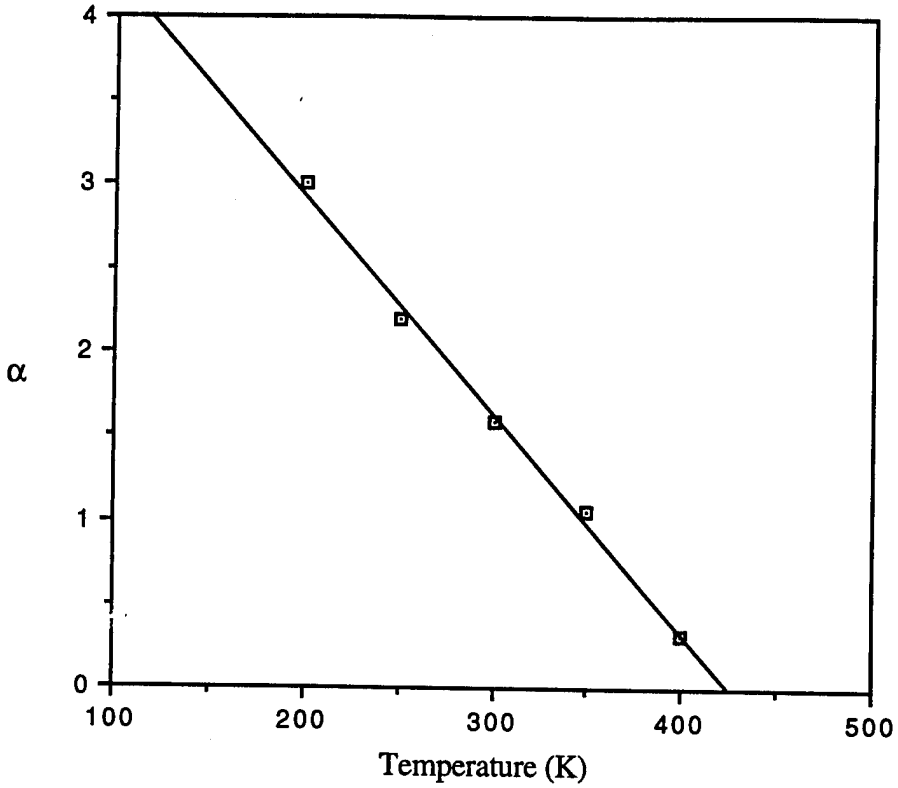

Figure 3. Enthalpy of condensation to ideal gas enthalpy ratio as a function of temperature.

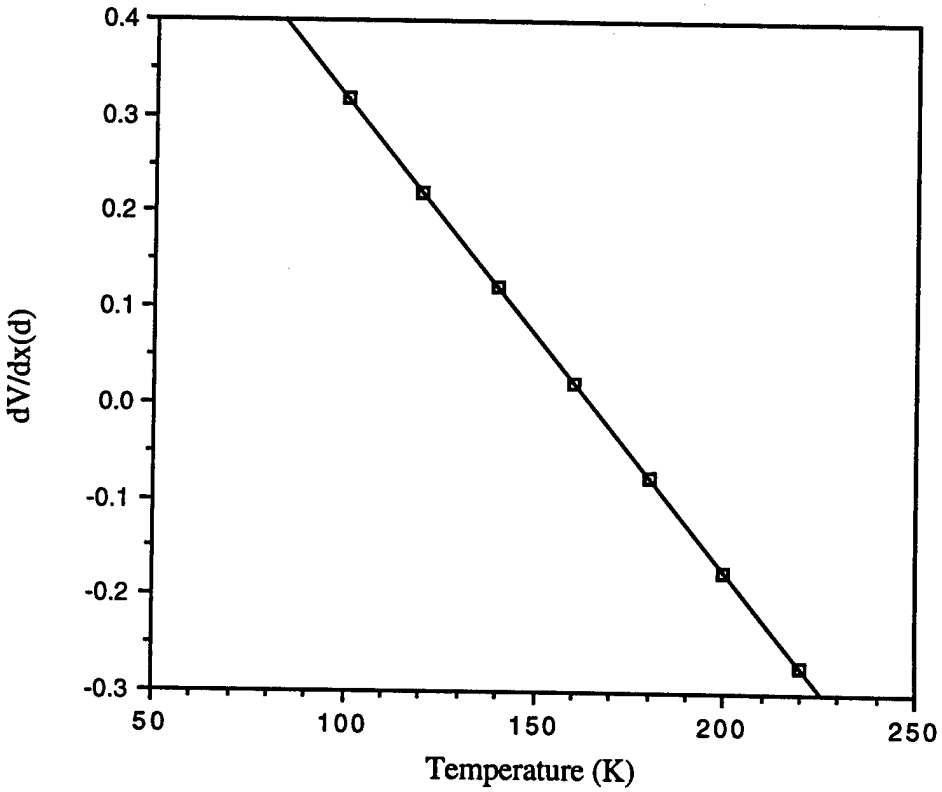

Figure 4. Velocity derivative with respect to dimer composition as a function of temperature.

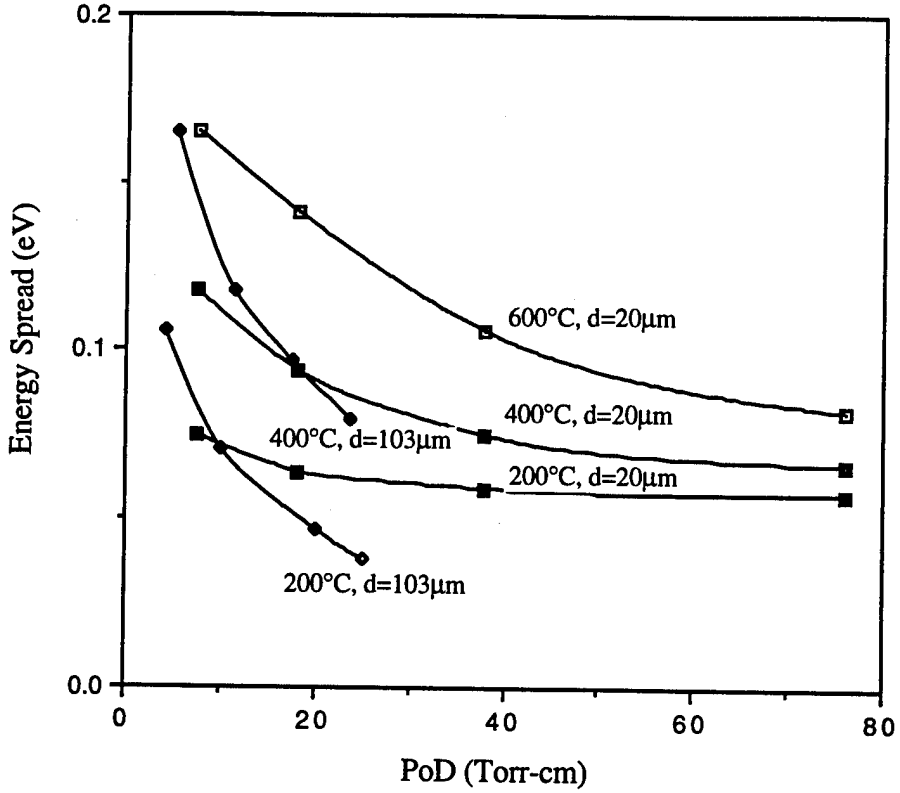

Figure 5. Energy spread as a function of the stagnation pressure-diameter product.

energy of the beams was found to increase with the stagnation temperature and pressure. Clustering plays a major role in determining the mean kinetic energy, as well as the energy spread. At 200°C clustering increases the energy of the beam whereas at 400°C it decreases the mean kinetic energy. The energy spread is higher for the LP series at low P_od. With increasing P_od, ΔE for the LP data is lower than that of the HP data. This is related to the amount of clustering which increases ΔE, the local temperature during clustering which determines the amount of enthalpy released and the efficiency of cooling which depends on the stagnation pressure and temperature.

F. Future Work

The molecular beam chamber described in previous reports as well as the supporting frame have been delivered. Testing of the chamber and preliminary depositions will be performed.

G. References

1. S. Strite and H. Morkoc, J. Vac. Sci. Technol., **B10**, 1237 (1992).
2. M. E. Jones, L. Q. Xia, N. Maity, J. R. Engstrom, Chem. Phys. Lett. **229**, 401 (1994).
3. S. T. Ceyer, J. D. Beckerle, M. B. Lee, S. L. Tang, Q. Y. Yang, M. A. Hines, J. Vac. Sci. Technol. a **5**, 501, Jul/Aug 1987.
4. D. R. Miller, *Atomic and Molecular Beam Methods*, Ch. 2, Ed. G. Scoles, 1988, Oxford University Press.
5. R. B. Doak and D. B. Nguyen, Progress in Astronautics and Aeronautics **117**, 187 (1989).

V. Electronic Structure Calculations

While most of the density-functional calculations for semiconductor materials are carried out under the assumption of the frozen-core approximation, it is known that the 3*d* electrons of Ga are not inert in all cases. Especially in GaN, the 3*d* states of Ga appear to be hybridized with the bottom *s*-like valence band stemming from N 2*s*. This results from the small energetic separation between the 3*d*-core states from the N 2*s*-level. Several approaches have been suggested to obtain a proper treatment of the Ga *d* shell.

Our initial calculations are focused on the construction of various pseudopotentials for Ga involving the core states by means of the non-linear core correction (NLCC) and additionally also be treating the 3*d* states as valence electrons. We use soft norm-conserving pseudopotentials in the form of [1, 2]. The potentials are tested by performing calculations for the static and vibrational properties of GaP and GaN using the plane-wave linear-response approach of Baroni and co-workers [3, 4].

Results indicate that the lattice constant for GaP in the zincblende-structure is slightly underestimated by about 3 percent if the effects of the 3*d* core are neglected while the underestimation is reduced to about 1 percent on the basis of the NLCC. A complete self-consistent treatment of the 3*d* states yields the best agreement of our results for GaP with experimental data both for the static properties as well as the calculated phonon frequencies.

Currently, the static and dynamic properties of GaN are calculated with the different potentials constructed for Ga. One aim is to obtain reliable results for GaN from theory by a proper treatment of the Ga 3*d* states. As many experimental results are still spread over a wide range especially for GaN, such calculations provide important information about the physical properties of the ideal material.

In the next step of the calculations, the *ab initio* tight-binding method based on the Harris functional is applied to the investigation of the growth properties of GaN. In that respect the results from the plane-wave calculation provide detailed information for a verification of the results obtained from the Harris total energy scheme and are useful as a guideline for a proper treatment of Ga and N in that approach.

References

1. G. B. Bachelet, D. R. Hamann und M. Schl"uter, Phys. Rev. B **26**, 4199 (1982).
2. N. Troullier und J. L. Martins, Phys. Rev. B **43**, 1993 (1991).
3. S. Baroni, P. Giannozzi und A. Testa, Phys. Rev. Lett. **58**, 1861 (1987).
4. P. Giannozzi, S. de Gironcoli, S. Baroni und P. Pavone, Phys. Rev. B **43**, 7231 (1991).

VI. Distribution List

Mr. Max Yoder Office of Naval Research Electronics Division, Code: 312 Ballston Tower One 800 N. Quincy Street Arlington, VA 22217-5660	3
Administrative Contracting Officer Office of Naval Research Regional Office Atlanta 101 Marietta Tower, Suite 2805 101 Marietta Street Atlanta, GA 30323-0008	1
Director, Naval Research Laboratory ATTN: Code 2627 Washington, DC 20375	1
Defense Technical Information Center Bldg. 5, Cameron Station Alexandria, VA 22304-6145	2